9 Particle physics with the CMS experiment at CERN

T. Årrestad, D. Brzhechko, L. Caminada, F. Canelli, A. de Cosa, P. Bärtschi, R. del Burgo, S. Donato, C. Galloni, M. Gienal, T. Hreus, St. Leontsinis, B. Kilminster, I. Neutelings, D. Pinna, G. Rauco, P. Robmann, D. Salerno, K. Schweiger, C. Seitz, Y. Takahashi, A. Zucchetta

in collaboration with: CMS - Collaboration

The CMS experiment acquired a record year of data in 2017, collecting over 50 fb^{-1} of proton-proton collisions with a center of mass energy of 13 TeV. A new pixel detector, built largely at UZH in collaboration with PSI and ETH, was installed in February 2017, just prior to this data taking period. This detector provided improved vertex resolution for primary and secondary production of charged particles, and higher hit efficiencies and rate capabilities.

Here we present an overview of our CMS activities. Our major activity in 2017 was calibrating and understanding the data from the new 4-layer Phase 1 pixel detector system. We have also begun design studies of a future pixel detector upgrade for the Phase 2 operation of the LHC (HL-LHC). Our group has taken responsibility for a pixel detector that will extend CMS tracking coverage to a more forward detector region; it is envisioned to be ready in 2024. Besides our work on the original and upgraded pixel detectors, we are also involved in trigger development and monitoring as well as physics data analysis on a number of different topics.

Our physics analysis program addresses fundamental questions in particle physics. After the discovery of a Higgs particle at the LHC [1], studies of its properties are among the primary goals. We are testing the fermionic couplings of the Higgs boson, with several analyses geared towards its couplings to tau leptons, top quarks, and bottom quarks. We are testing several theoretical models which could extend the Standard Model (SM), by directly searching for new particle states of mass up to 4 TeV. These generate loop corrections with the necessary cancellations to stabilize the Higgs boson mass. Models such as supersymmetry (SUSY), extra dimensions, and vector-like quarks justify the low Higgs boson mass, and predict a wide range of new particles, which we are sifting through CMS data to observe. We have also begun a new analysis program, testing for violations of lepton flavor universality.

Members of our group play important coordination roles. In the period covered by this report, S. Donato lead the High Level Trigger (HLT) group. C. Seitz acted as subgroup convener within the inclusive SUSY physics group. A. de Cosa led the pixel monitoring group, and was subgroup convener within the Beyond 2 Generations physics group, C. Galloni was convener of the tau lepton identification group. S. Donato and L. Caminada are members of the Swiss Tier 3 computing steering committee. F. Canelli is on the CMS Management Board, and B. Kilminster is on the Management Board for the Phase 2 upgrade and the Tracker group.

[1] ATLAS collaboration, Phys. Lett. B **716** (2012) 29; CMS collaboration, Phys. Lett. B **716** (2012) 30.

9.1 The CMS experiment

CMS [2] is one of the multipurpose detectors at the LHC. It consists of different layers of detectors optimized for position and energy measurements of particles produced in collisions. An all-silicon tracker, an electromagnetic calorimeter, and a hadronic sampling calorimeter are all contained within a large-bore 3.8 T superconducting solenoid. Beyond the solenoid there are four layers of muon detectors. The CMS tracker is composed of the inner pixel detector and the outer silicon strip detector. The upgraded pixel detector, installed in 2017, consists of four barrel layers (BPIX) at 2.9, 6.8, 10.9, and 16.0 cm, and three forward/backward disks at longitudinal positions of $\pm$32, 36, and 46 cm, and extending in radius from about 6 to 15 cm. The high segmentation of the pixel detector allows for high-precision tracking in the region closest to the interaction point. The pixel detector information is crucial for primary vertex and pile-up vertex reconstruction, and identification of long-lived τ-leptons and B-hadrons. The performance of this newly installed pixel detector has been excellent. The barrel pixel detector was built with major contributions from the Swiss Consortium of PSI, ETH and the University of Zurich.

[2] CMS collaboration, JINST **3** (2008) S08004.

9.2 Detector maintenance and operation

The pixel detector is a central component in the reconstruction of high-quality data used in CMS physics anal-

yses. With more than 100 million channels, it provides most of the data of the CMS experiment, allowing precise tracking of charged particles near the point of their creation. Our group made significant contributions to the operation of the pixel detector as well as the re-calibration during technical stops of the accelerator. We are responsible for the monitoring of detector performance and operational parameters, which are crucial in order to respond with preventive actions that ensure high-quality data.

In particular, we keep track of the evolution of the radiation damage to the silicon sensors with increasing luminosity, measuring threshold and noise distributions, as well as pixel hit resolutions, and determine the impact of dynamic inefficiencies in the pixels. As responsible for monitoring the effect of radiation on the health of the pixel detector, we developed a robust system to verify the evolution of the leakage current in the silicon sensors as a function of the integrated luminosity, and hence, on the radiation dose absorbed by the system. Figure 9.1 shows how the leakage current circulating in the sensors increases with the increase in integrated luminosity, for the four barrel layers. The pixel hit resolution of all regions of the pixel detector is studied to verify the detector is operating optimally and the reconstruction parameters are properly set (see Fig. 9.2).

During the last two months of 2017 operation, an issue with the DC-DC converters used in the power system of the pixel detector occurred. An increasing number of DC-DC converters failed, such that 67 out of 1128 converters were unresponsive by the end of the run. In order to investigate the problem and ensure the best possible performance during 2018, the pixel system was extracted for repair in the technical stop at the end of 2017. Within less than a month, we were able to replace all DC-DC converters with new components, substitute modules in the innermost layer that had been damaged as a consequence of the DC-DC converter failure, and resolve system-level

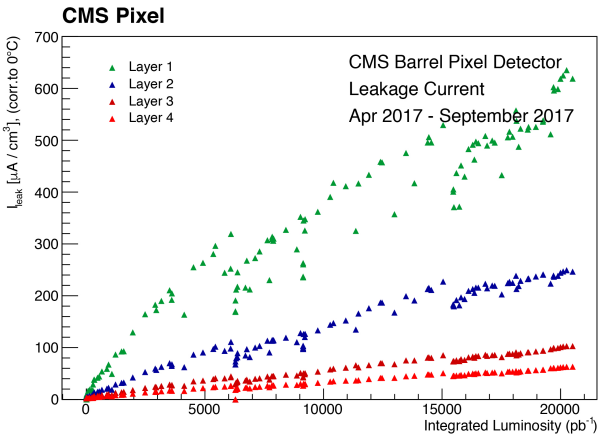

FIG. 9.1 – The CMS Phase 1 pixel detector leakage current per unit of silicon volume for the four barrel layers as a function of the integrated luminosity.

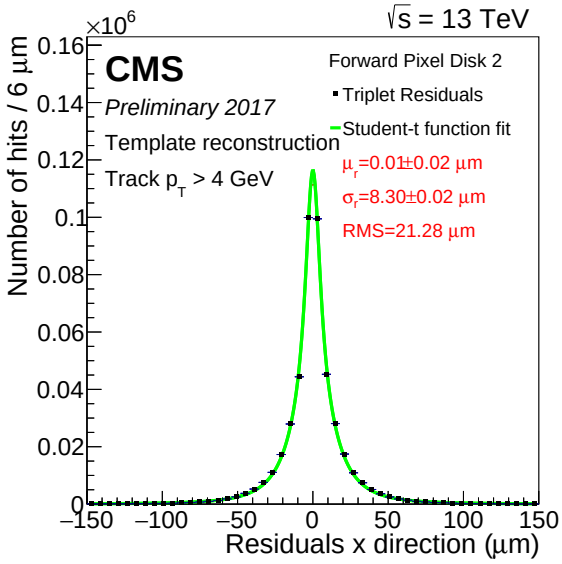

FIG. 9.2 – Resolution in transverse direction of one of the disks of the pixel detector with 2016 data, as determined by interpolating tracks through layers of the detector.

problems with individual power and readout groups that had prevented some fraction of the detector (4%) from being operational in 2017. At the beginning of March 2018 we reinstalled the pixel detector in CMS and our effort on commissioning, and calibration was completed in time to record the first data of 2018. The performance of the DC-DC converters is being closely monitored and preventive measures have been put in place to mitigate potential losses. Figure 9.3 shows UZH and PSI members replacing DC-DC converters at CMS. It has since been determined that the problem is due to a defect in the CERN chip responsible for controlling

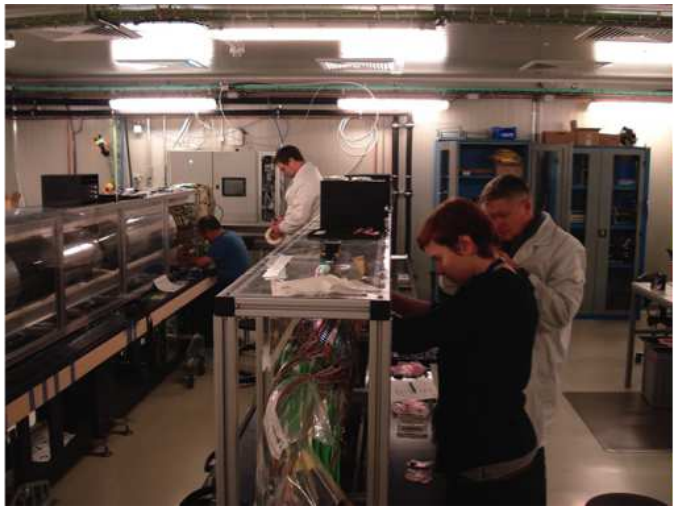

FIG. 9.3 – Replacement of BPIX DC-DC convertors in clean room at surface of CMS experimental area by UZH and PSI members in early 2018.

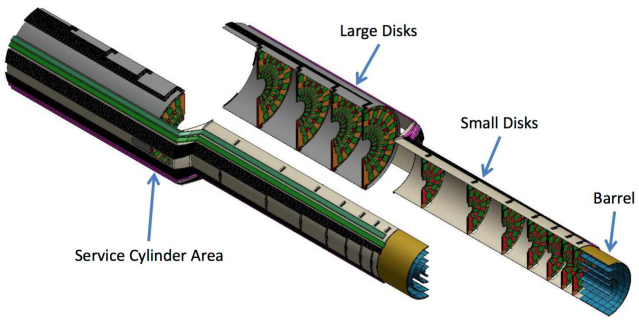

FIG. 9.4 – A quarter of the proposed phase 2 pixel detector for the CMS upgrade. The detector barrel section is composed of four cylindrical layers, while the forward region is composed of seven small disks and four large disks.

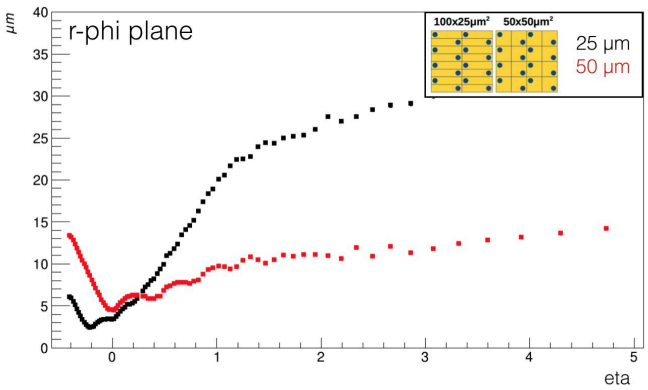

FIG. 9.5 – Resolution (r-ϕ vs η) of different simulated pixel sizes for the phase 2 pixel detector.

the DC-DC converter, and the CERN microelectronics group has now developed a fix, so that we will again replace all the DC-DC converters at the end of 2018.

Our group is also involved in another key part of the CMS detector, the HLT system. One group member is in charge of the group dedicated to the trigger menu integration and trigger code development in the HLT. The main responsibility is to guarantee that the trigger software works properly, and to keep it updated with the changes proposed by the physics analysis groups. This task is very important since any error in the trigger might compromise the data taking of the whole CMS experiment. Our group also monitors and studies the online performance of the triggers that include b-tagging, these are crucial in many physics analyses in CMS.

9.3 Upgrades

The upgraded pixel detector is designed to provide optimal performance for the whole Phase 1 operation, until the third long shutdown of the accelerator (2023-2025), when a new pixel detector for the High Luminosity LHC (HL-LHC) will be installed (Phase 2). The Phase-2 CMS pixel detector is composed of three parts, a barrel detector and two detectors composed of disks. The UZH CMS group will be constructing the large disk detectors (see Fig. 9.4). To meet the challenges arising from the increased luminosity of the machine, we are already now performing R&D for the next generation of pixel systems. In particular, efforts are ramping up to evaluate the performance of different designs concerning the number and positioning of the pixel layers, the optimal pixel size as well as the overall mechanical design and technical implementation. We have studied different geometries of Phase 2 pixel detector sensors by fully simulating the relative angles of particles reaching the detector, the drift of electrons and holes, the effect of the CMS magnetic field, as well as digitization and clustering. Some results are shown in Fig. 9.5, and have been used to optimize the detector pixel sizes. Our group is also researching the possibility to add a layer of tracking that can also provide precise timing resolution, in order to reduce pileup and identify Higgs boson production with forward jets. We are currently testing the timing resolution of low gain avalanche diode sensors (LGADs) with sources as shown in Fig. 9.6. The ultimate sensitivity we hope to achieve is to measure the time a charged particle passes through the detector with a timing resolution of 30 ps.

9.4 Higgs Properties

9.4.1 Higgs boson couplings to top quarks

The Higgs boson couples strongly only to the top quark. The search for the Higgs boson produced in association with a top-quark pair ($t\bar{t}H$) is the only way to directly probe this coupling and, among $t\bar{t}H$ channels, the

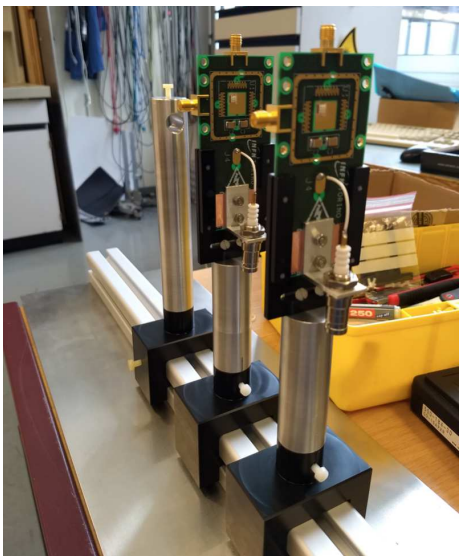

FIG. 9.6 – Part of a setup for testing the timing resolution of LGAD sensors for the Phase-2 CMS pixel detector with a radioactive source.

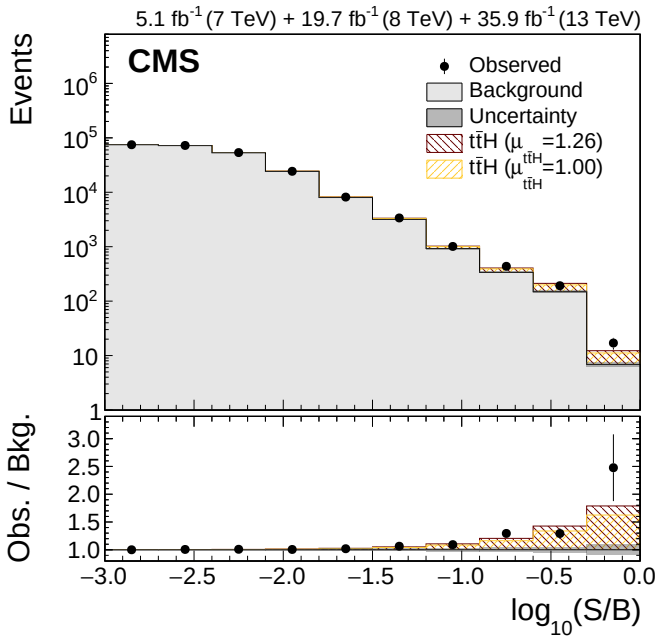

FIG. 9.7 – Observation of $t\bar{t}H$ by the CMS collaboration. The shaded histogram shows the expected background distribution, with different signal hypotheses considered shown stacked on the background. In the SM, the multiplier of the expect signal is $\mu_{t\bar{t}H} = 1$, while the best fit signal is observed to be 1.26. The lower panel shows the ratios of the expected signal and observed results relative to the expected background.

search for the Higgs boson decaying into b quarks probes the largest Higgs branching ratio of $H \to bb$ ($\sim$ 58%), and its measurement allows a constraint purely on third-generation Higgs boson couplings.

One achievement this year has been to analyze fully-hadronic $t\bar{t}H$ final states of only quarks. Although this final state represents the largest branching ratio, it is the most challenging analysis due to the large contamination from SM background processes. After events are selected, a jet-based quark-gluon discriminator is used in an event-based likelihood ratio to differentiate between events containing jets originating from light-flavour quarks and events containing jets from gluons. Finally, a matrix element method (MEM) is used for optimal discrimination between the $t\bar{t}H$ signal and SM background processes and for the ultimate signal extraction.

The results of the fully hadronic $t\bar{t}H$ analysis [3] were included in the overall $t\bar{t}H$ combination at CMS [4] of all individual final-state searches of the Higgs boson performed at CMS at centre-of-mass energies of 7, 8 and 13TeV. The combination provides the first-ever observation of $t\bar{t}H$ production, with an observed significance of 5.2 standard deviations, and the most precise measurement of the $t\bar{t}H$ cross section to date, with a best fit signal strength of $\hat{\mu} = 1.26^{+0.31}_{-0.26}$, see Fig. 9.7. Without the fully-hadronic search, the measurement would have

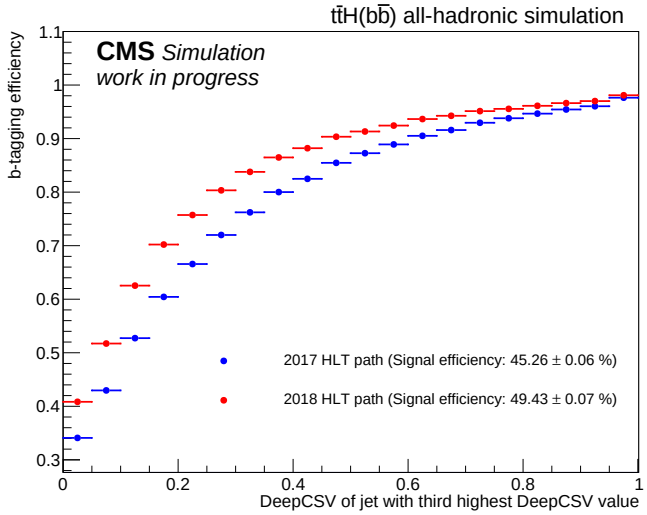

FIG. 9.8 – Improvement in the b-tagging efficiency for $t\bar{t}H(b\bar{b})$ fully-hadronic analysis made possible by utilizing a new HLT path with an improved b-tagging algorithm.

fallen short of the 5 standard deviations required to claim an observation [5].

With this measurement already made, we are now improving the future data sample size by optimizing the trigger selection of $t\bar{t}H$ events as in Fig. 9.8. We have also started a measurement of the $t\bar{t} + b\bar{b}$ inclusive cross section in the all-hadronic channel, which represents a large background for our search, and have developed new methods to reduce the QCD multijet background using a combination of two different boosted decision trees. The first results of these new methods are summarized in Table 9.1, that shows the yields of the expected signal and background processes after using our background rejection methods.

[3] CMS collaboration, arXiv:1804.03682 submitted to JHEP.

[4] CMS collaboration, Phys. Rev. Lett. 120 (2018) 231801.

[5] D. Salerno, CERN-THESIS-2018-026

Process	Yields
Other backgrounds	50100±300
Multijet	31000±200
Total bkg.	81100±400
$t\bar{t} + b\bar{b}$	8000±100
S/B	0.09
Data	89350

TAB. 9.1 – Expected yields for signal and backgrounds for the $t\bar{t} + b\bar{b}$ cross section measurement using 35.9 fb^{-1} of data collected by the CMS experiment in 2016, with statistical uncertainties.

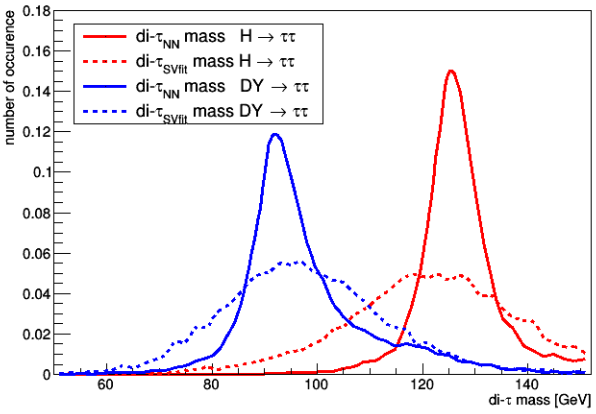

FIG. 9.9 – Improvement in the mass resolution using our Neutral Network (NN) algorithm compared to the default SVfit method used for the Higgs observation. The improvement is shown both for reconstructed Higgs bosons as well as Drell Yan (DY) events, which peak at the Z boson mass.

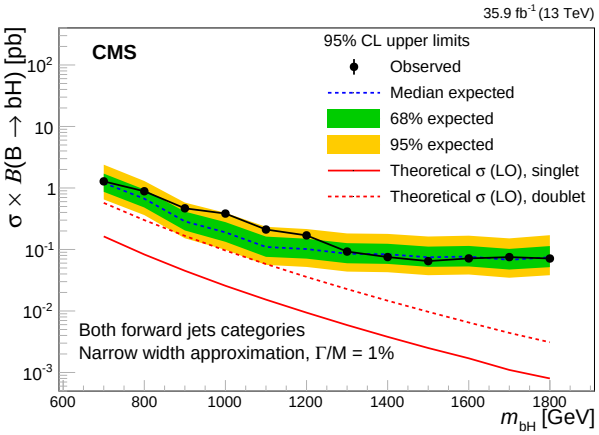

FIG. 9.10 – Results of a search for the single production of vector-like quarks B that decay to a b quark and a Higgs boson in fully-hadronic events with highly-boosted topologies. Upper limits at the 95% CL are set on the product of the B quark production cross section and branching fraction as a function of the signal mass, assuming narrow-width resonances of the resonance mass for the B quark.

9.4.2 Higgs boson coupling to τ leptons

In 2016, our CMS group reported the first observation of the Higgs boson decaying to tau leptons, for which we contributed to the analysis, the tau identification and scale factors, and as main editors of the observation publication [6]. We have now developed a new algorithm for improving the mass reconstruction of Higgs bosons decaying to tau leptons. Since tau leptons produce unmeasurable neutrinos in their decays, the Higgs boson mass is not fully constrained, therefore, a special algorithm (SVfit) has been traditionally used to calculate the most probable Higgs boson candidate mass. Using a machine learning algorithm, we have been able to greatly improve the mass resolution with respect to SVfit for particles decaying into two tau leptons, as shown in Fig. 9.9.

9.5 Searches for new phenomena

Our group is mainly focused on searching for new physics beyond the SM (BSM). We search for natural extensions that can solve inadequacies of the SM, such as its failure to predict a dark matter (DM) candidate, and its inability to explain the exceptionally low mass of the Higgs boson. We consider additional symmetries and extra dimensions that predict new particles, and also search for DM produced in our detectors. A new area of research in this period has been to directly probe for particles that may explain anomalies seen in indirect measurements seen with the LHCb experiment and other experiments focusing on b-quark physics.

9.5.1 Search for vector-like quarks

Many extensions of the SM, such as composite Higgs, extra dimensions, and little Higgs, predict the existence of a new class of heavy quarks, named vector-like quarks (VLQ) The existence of such particles would represent a solution to the hierarchy problem. Single electroweak production of VLQs has not yet been well-explored, despite the production being dominant above masses of 700 GeV. Our group has made a significant impact in the search for singly produced VLQs, carrying out two different searches, looking for massive B and T VLQs. Our focus is on two specific final states: $T \to tZ \to bq\bar{q}\nu\nu$ and $B \to bH \to bb\bar{b}$.

These new heavy resonances may decay into highly boosted quarks and bosons, whose decay products are merged into a unique “fat" jet, for which we use special techniques for identification. Our search for a vector-like quark particle, B, has been performed with an integrated luminosity of 35 fb^{-1} delivered by the LHC in 2016 and recently published [7]. The search focused on the hadronic final state of $B \to bH \to bb\bar{b}$ production channel. Advanced techniques of boosted Higgs boson production identification have been employed together with data-based methods to estimate background contributions. For the first time, in addition to narrow widths resonances, more realistic scenarios of resonance widths corresponding to 10, 20 and 30% of the resonance mass have been investigated. Results of the search are shown in Fig 9.10.

[6] A. M. Sirunyan *et al.* [CMS Collaboration], Phys. Lett. B **779**, 283 (2018), arXiv:1708.00373.

[7] CMS collaboration, JHEP 06 (2018) 031.

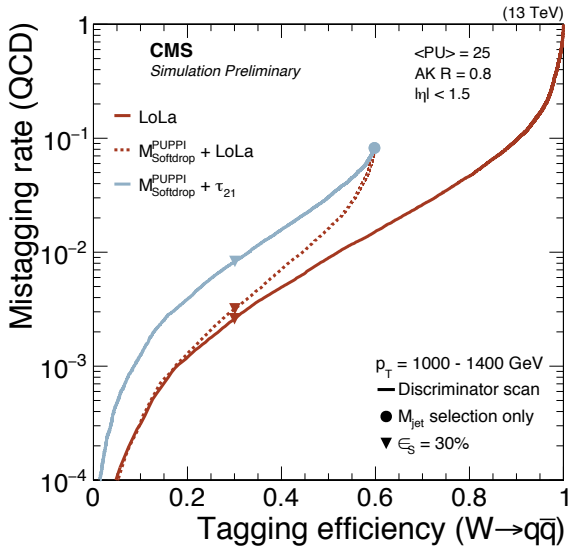

FIG. 9.11 – Performance of the LoLa algorithm for identifying boosted, hadronically-decaying bosons, as compared to the standard algorithm of PUPPI and Softdrop. Shown are curves comparing the efficiency for tagging a signal W-boson jet with the probability for mistagging a QCD-produced jet.

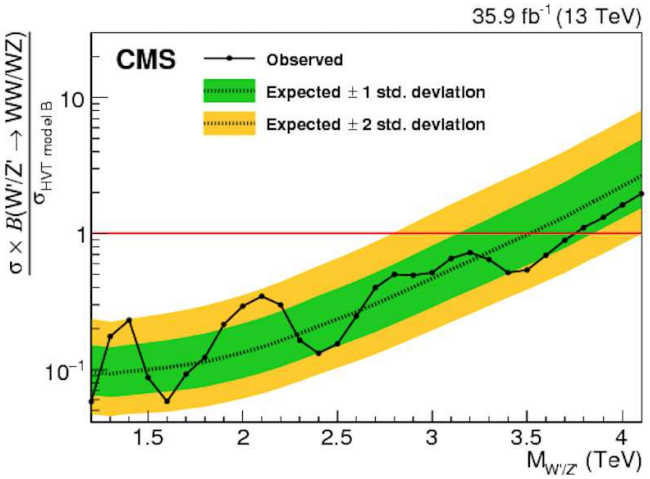

FIG. 9.12 – 95% exclusion bounds on the signal strength (product of theoretical cross section and the branching fraction to WW and ZZ) for spin-1 particles predicted by the triplet hypothesis of the HVT model B.

9.5.2 Search for heavy resonances in diboson events

The UZH group plays a leading role in searches for heavy resonances, with masses larger than 1 TeV, decaying into a pair of SM bosons (W, Z, or the Higgs boson). These heavy resonances are predicted by a large number of theoretical models that extend the SM and provide an explanation for the hierarchy problem. The most credited theories include extra dimensions, composite Higgs, heavy vector-triplets, and additional $U(1)$ gauge groups [8]. These models predict the presence of massive spin-0 Radions, spin-2 Gravitons, or spin-1 heavy W' or Z' bosons which may decay with a significant branching fraction into SM bosons.

As a consequence of the heavy mass of the new particles, and the large Lorentz boost of the decay products, the pair of particles originating from the decay of the SM bosons usually have a small angular separation and special identification and reconstruction techniques must be employed. We have designed a new machine-learning algorithm for identifying boosted bosons, called LoLa, which provides an improvement in identification efficiency over the standard tagging algorithm that uses PUPPI [9] and Soft Drop [10] (see Fig. 9.11).

During the last year, our group produced several new results using the 2016 dataset, which was a factor of 5 larger than the previously available dataset of 13 TeV center-of-mass collisions. Using events identified as containing hadronically-decaying boosted jets, where we have the largest statistics, we are able to search for heavy resonances, and interpret them as bulk gravitons, heavy vector triplet W′ and Z′ resonances, and excited quarks. We have set upper limits on the cross sections for such particles, for masses up to 5.0 TeV [11]. Figure 9.12 shows constraints on one of these models. We have also searched for new particles decaying to a W or Z boson and a Higgs boson, such that the Higgs boson is boosted and decays into b quarks that are overlapping in a single jet. Our search considers events in which the W or Z bosons decay leptonically into zero, one, or two leptons (see Fig. 9.13).

Beyond this, we have searched for a high mass resonance decaying to two Higgs bosons ($X \to HH \to b\bar{b}\tau^-\tau^+$). Our new results using the 2016 dataset extend the search range for such particles up to 4 TeV, and a publication is in its final stages of review within CMS. The results put constraints on BSM radion particles, as shown in Fig. 9.14. The preliminary result [15] is almost fully reviewed and expected to be submitted for publication in the next month.

[8] K. Agashe *et al.*, Phys. Rev. D **76** (2007) 036006;
L. Randall, R. Sundrum,
Phys. Rev. Lett. **83** (1999) 3370;
D. Marzocca *et al.*, JHEP **08** (2012) 013;
R. Rattazzi *et al.*, JHEP, 2011(10), 2011;
D. Pappadopulo *et al.*, arXiv:1402.4431.

[9] D. Bertolini *et al.*, JHEP **2014** (2014) 59.

[10] A. J. Larkoski *et al.*, JHEP **05** (2014) 146.

[11] A. M. Sirunyan *et al.* [CMS Collaboration], Phys. Rev. D **97**, no. 7, 072006 (2018), arXiv:1708.05379.

[12] CMS Collaboration, CMS-PAS-B2G-17-004.

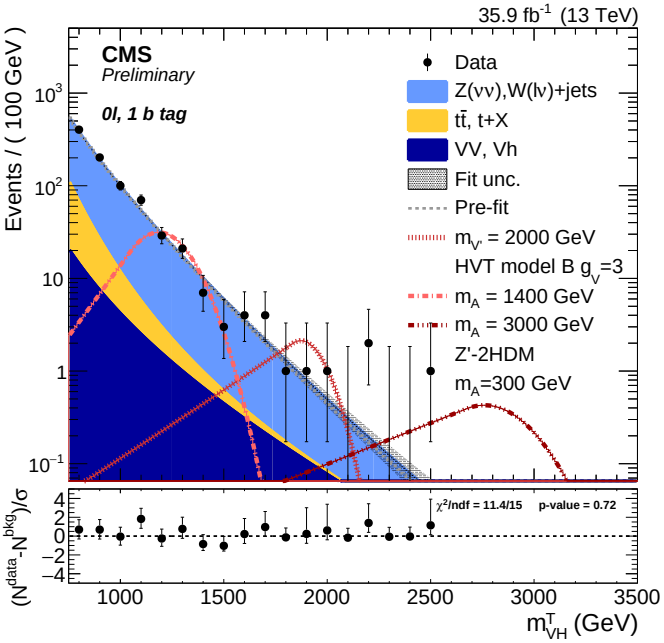

FIG. 9.13 – Observed data in the 0 lepton, 1 b-tag category. The filled areas represent the contribution of the main backgrounds (W, Z + jets, $t\bar{t}$, SM diboson). The dotted lines represent the different beyond-the-SM signal hypotheses tested: a heavy Z' that decays to a Z and a Higgs boson, or a heavy Z' that decays in a Higgs boson and DM particles, the latter mediated by a heavy pseudoscalar boson (Z'-2HDM model).

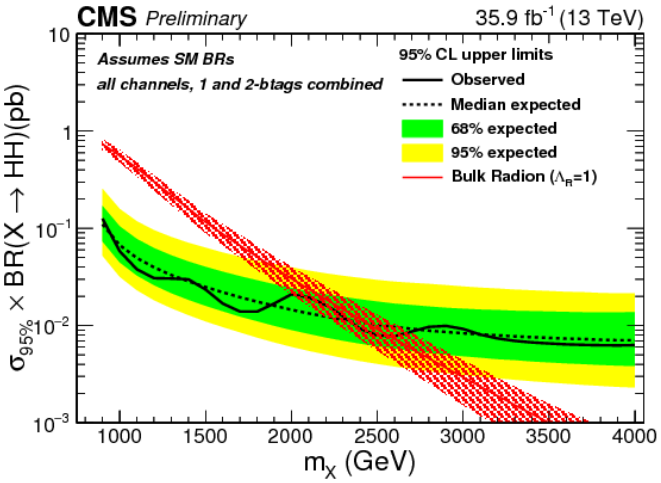

FIG. 9.14 – Observed 95% CL upper limits on $\sigma\,\mathcal{B}$(X(spin-0)→HH). Expected limits are shown with ±1 and ±2 standard deviation uncertainty bands. The $\ell\tau_h$ and $\tau_h\tau_h$ final states, and one and two b-tagged sub-jet categories are combined in the limits. The solid line and the dashed area correspond to the cross sections predicted by the radion model and the related theoretical uncertainties.

[13] A. M. Sirunyan *et al.* [CMS Collaboration], Eur. Phys. J. C **77**, no. 9, 636 (2017), arXiv:1707.01303.

[14] A. Zucchetta [CMS Collaboration], PoS DIS **2017**, 286 (2018).

[15] CMS Collaboration, CMS-PAS-B2G-17-006.

9.5.3 Supersymmetry (SUSY)

One of the favored extensions of the SM is SUSY, predicting a variety of new particles at the TeV scale, that differ in spin from their SM counterparts. SUSY provides an elegant solution to some of the shortcomings of the SM, including the hierarchy problem and the nature of DM.

One SUSY model describes the pair production of gluinos, where each gluino decays into two top quarks and the lightest supersymmetric particle, which does not interact and escapes detection. Our group has been part of the efforts to search for this type of decay in the exclusive single lepton final state, which has the advantage of a large branching ratio and a fairly clean SM background, mainly originating from top quark pair production with additional jets. Multiple exclusive search regions are defined, by binning events in various kinematic variables. The observed data in each of these regions is compared with the expected SM background, which is estimated by data driven techniques. We observe good agreement between the prediction and data and can place limits on the gluino pair production cross section as a function of neutralino and gluino mass, as shown in Fig. 9.15. The results are based on the full dataset of 35.9 fb^{-1} collected during 2016 and have been published in [16] and [17]. Gluino masses are excluded up to 1800 GeV.

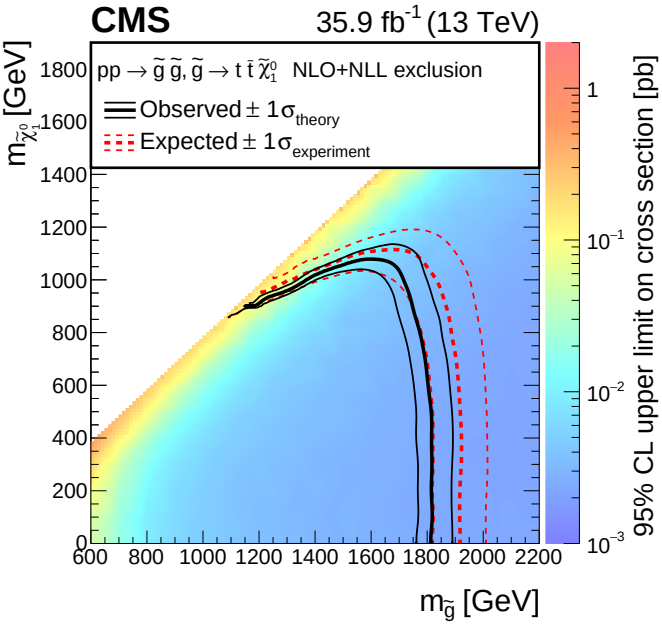

FIG. 9.15 – The results of a supersymmetric search, shown as limits on the gluino pair production cross section as a function of the neutralino and gluino masses. Gluino masses can be excluded up to 1800 GeV.

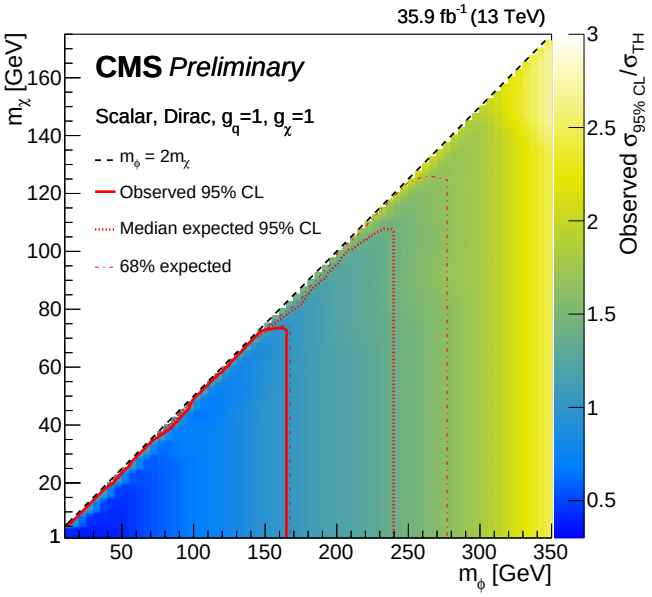

FIG. 9.16 – Results on the search for DM produced in association with a top quark pair. Expected and observed 95% CL upper limits are shown on the ratio of the DM production cross section to the model expectation as a function of the scalar mediator mass (m_{MED}), with the single-lepton and fully-hadronic channels combined. A DM mass of 1 GeV is assumed [19].

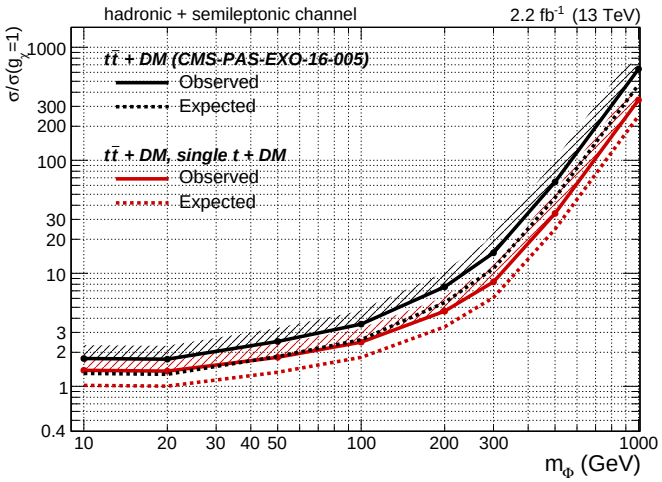

FIG. 9.17 – Comparison between the expected and observed exclusion limits on the signal strength by considering the contribution of the single top quark and DM production summed to the top quark pair production, as originally considered by CMS. A significant improvement in sensitivity is observed when considering the new DM production mechanism.

[16] CMS Collaboration, *Phys. Lett. B* 780 (2018) 384.

[17] CMS Collaboration, *Phys. Rev. D* 95, 012011 (2017).

9.5.4 Search for dark matter particles with top quarks

In several new physics models, a weakly interacting massive particle arises naturally as a DM candidate. So far, however, there is no established knowledge about its properties and interactions with ordinary matter. DM may couple to matter in proportion to mass, leading to DM being produced with top quarks at the LHC [18].

The DM particle would escape detection, therefore the signature of this type of event is large missing energy recoiling against the top quarks. Our group has made a significant impact on this search with 8 TeV and the 13 TeV data collected in 2015, the latter was published in 2017 [19]. We have developed a new and improved analysis, for which we had performed detailed studies of the different model parameters in the context of simplified models, namely the couplings strengths involved and the dependency of the analysis sensitivity on different DM and mediator mass hypotheses. Results with an integrated luminosity of 35 fb^{-1} delivered by the LHC in 2016 are shown in Fig. 9.16. Preliminary results can be found at [20], and a journal publication is currently in preparation. In addition to top quark pairs, DM can also be produced in association with a single top quark [21], [22]. Our group discovered this alternate signal mechanism, and previously produced a phenomenology paper discussing its improvement in sensitivity. This year, the analysis was developed and applied to CMS data, and is expected to become public in 2018. We have found that the exclusion limits can be improved by $30-90\%$ by including the single top quark processes, depending on the assumed scalar mediator mass, as can be seen in Fig. 9.17.

[18] D. Abercrombie *et al.*, arXiv:1507.00966.

[19] CMS collaboration, Eur. Phys. J. C 77 (2017) 845.

[20] CMS collaboration, CMS-EXO-16-049.

[21] D. Pinna *et al.*, arXiv:1701.05195.

[22] D. Pinna, CERN-THESIS-2017-211

9.5.5 Search for leptoquarks

The LHCb experiment and other dedicated B physics experiments have reported an increasing set of experimental anomalies in semi-leptonic B-meson decays, appearing in both charged and neutral currents. Ongoing work to solidify the understanding of these effects is reported by LHCb in Section 8. The particle physics community is now confronting these two 4σ deviations from the SM [23, 24]. The UZH theory group has brought forth

some interesting BSM models to explain these anomalies with new particles called leptoquarks that have an enhanced coupling to third generation particles, as explained in Section 2. In the past year, our CMS group has searched directly for these particles, considering events in which a hypothetical, third-generation leptoquark is produced singly, decaying to a tau lepton and b quark. Since the single production cross section of leptoquarks grows with the Yukawa coupling λ at the LQ-lepton-quark vertex, it can extend the mass range of leptoquark searches at high values of λ. Results of this search are shown in Fig. 9.18, and have been submitted for peer review for publication.

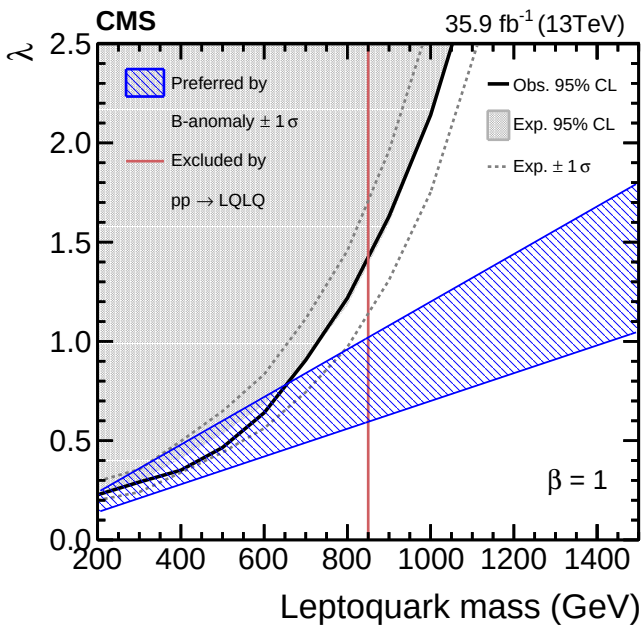

FIG. 9.18 – The red line shows the 95% CL upper limit of leptoquark masses excluded through searches for LQ-pair production, while the black (gray) line shows the 95% CL observed (expected) upper limit on singly-produced leptoquarks, as a function of the Yukawa coupling λ at the LQ-lepton-quark vertex. The blue band represents the range of mass and coupling preferred by B anomalies .

[23] Y. Amhis *et al.*, Heavy Flavor Averaging Group, "Averages of b-hadron, c-hadron, and τ-lepton properties as of summer 2016," arXiv:1612.07233.

[24] W. Altmannshofer and D. M. Straub, "Implications of $b \to s$ measurements," arXiv:1503.06199.